Chem. Res. Chin. Univ., 2015, 31(2), 187—191 doi: 10.1007/s40242-015-4316-y

A Series of Lanthanide Coordination Polymers Constructed from 4-Pyridin-4-ylbenzoate

FANG Weihui and YANG Guoyu*

State Key Laboratory of Structural Chemistry, Fujian Institute of Research on the Structure of Matter, Chinese Academy of Sciences, Fuzhou 350002, P. R. China

Abstract Four lanthanide coordination polymers, $LaL_3(H_2O)_2$(**1**), $LnL_2(\mu_3\text{-}OH)(H_2O)$[Ln=Eu(**2**),Tb(**3**)] and $ErL_3{\cdot}2H_2O$(**4**) were synthesized *via* hydrothermal reactions of lanthanide oxide with 4-pyridin-4-ylbenzonic acid(HL), and characterized by means of elemental analyses, infrared(IR) spectrometer, powder X-ray diffraction(PXRD), thermogravimetric analyses(TGA) and single-crystal XRD. The results reveal that complex **1** possesses a linear chain structure, complexes **2** and **3** possess isostructural ladder-like chains, while complex **4** possesses a 2D layer with 4-connected *sql* topology. Furthermore, the luminescence properties and UV-Vis spectra of complexes **2** and **3** were investigated.

Keywords Hydrothermal synthesis; Lanthanide; Luminescence property

1 Introduction

Coordination polymers(CPs) are a promising class of crystalline complexes with fascinating structures and wide applications[1]. With regard to lanthanide(Ln) CPs[2], they have attracted increasing attention in the fields of luminescence[3,4], magnetism[5] and catalysis[6], etc. However, compared to the coordination chemistry of transition metals(TMs), the analogue chemistry of Ln has been still underdeveloping for its high coordination numbers, flexible coordination environment and unpredictable network topologies. At present, a common synthetic strategy is to control the hydrolysis of Ln salts in the presence of supporting ligands. Thus, the judicious choice of supporting ligands is particularly important. In our previous work, by employing isonicotinic acid(HIN) and nicotinic acid (HNA), a series of Ln-TM CPs has been achieved[7—9]. Though coordination chemistry of HIN and HNA has been well documented[10], analogue ligands of 4-pyridin-4-ylbenzoic acid(HL)[11] and 4-pyridin-3-ylbenzoic acid(HL′)[12] to Ln CPs have less been reported. Based on our primary studies[13—15], a series of chain and layered Ln CPs{$LaL_3(H_2O)_2$(**1**), $LnL_2(\mu_3\text{-}OH)(H_2O)$[Ln=Eu(**2**), Tb(**3**)] and $ErL_3{\cdot}2H_2O$(**4**)} was reported in this paper. Complex **1** exhibited linear chain structure, complexes **2** and **3** were ladder-like chains and complex **4** had a 2D layered network. Notably, red and green luminescence of complexes **2** and **3** was observed.

2 Experimental

2.1 Materials and Measurements

All the chemicals were analytical reagents. The elemental analysis was carried out by the combustion method on an Elemental Vario EL III CHNOS elemental analyzer. Powder X-ray diffraction(PXRD) data were collected on a Rigaku Mini Flex II diffracometer using Cu $K\alpha$ radiation(λ=0.154056 nm) under ambient conditions. Infrared(IR) spectra(KBr pellet) were recorded on an ABB Bomen MB102 spectrometer over a wavenumber range of from 400 cm^{-1} to 4000 cm^{-1}. The thermogravimetric analyses(TGA) were performed on a Mettler Toledo TGA/SDTA 851^e analyzer in air atmosphere with a heating rate of 10 ºC/min from 30 ºC to 1000 ºC. Photoluminescence analyses were performed on an Edinburgh Instrument F920 fluorescence spectrometer.

2.2 Syntheses

2.2.1 Synthesis of $LaL_3(H_2O)_2$(1)

A mixture of La_2O_3(0.3 mmol, 98 mg), HL(0.5 mmol, 100 mg), H_2O(10 mL, 0.22 mmol) and 0.5 mol/L H_2SO_4 with the pH value of about 2.0 was sealed in a 30 mL Teflon-lined bomb at 200 ºC for 3 d, and then cooled to room temperature. After filtration, washed with distilled water and dried at ambient temperature, pink crystals of complex **1** were recovered(yield 17% based on La_2O_3). Elemental analysis(%) calcd. for $C_{36}H_{28}LaN_3O_8$(**1**): C 56.19, H 3.67, N 5.46; found: C 55.56, H 4.17, N 5.41.

2.2.2 Synthesis of $LnL_2(\mu_3\text{-}OH)(H_2O)$[Ln=Eu(2), Tb(3)]

A mixture of Ln_2O_3(Eu_2O_3: 0.3 mmol, 106 mg; Tb_4O_7: 0.15 mmol, 112 mg), HL(1 mmol, 199 mg), H_2O(10 mL, 0.22 mmol) and 0.5 mol/L H_2SO_4 with the pH value of about 2.0 was sealed in a 30 mL Teflon-lined bomb at 190 ºC for

*Corresponding author. E-mail: ygy@fjirsm.ac.cn

Received August 25, 2014; accepted November 28, 2014.

Supported by the National Natural Science Foundation of China(Nos.91122028, 21221001, 50872133) and the National Basic Research Program of China(Nos.2014CB932101, 2011CB932504).

3 d, and then cooled to room temperature. After filtration, washed with distilled water and dried at ambient temperature, yellow crystals of complexes **2** and **3** were recovered(yield 31% based on Eu_2O_3; yield 34% based on Tb_4O_7). Elemental analysis(%), calcd. for $C_{24}H_{19}EuN_2O_6$(**2**): C 49.41, H 3.28, N 4.80; found: C 49.24, H 3.32, N 4.89; calcd. for $C_{24}H_{19}TbN_2O_6$(**3**): C 48.83, H 3.24, N 4.74; found: C 48.84, H 3.28, N 4.83.

2.2.3 Synthesis of $ErL_3{\cdot}2H_2O$(4)

A mixture of Er_2O_3(0.5 mmol, 191 mg), HL(2 mmol, 398 mg), H_2O(10 mL, 0.22 mmol) and 0.5 mol/L H_2SO_4 with the pH value of about 2.0 was sealed in a 30 mL Teflon-lined bomb at 170 ºC for 10 d, and then cooled to room temperature. After filtration, washed with distilled water and dried at ambient temperature, pink crystals of complex **4** were recovered(yield 46% based on Er_2O_3). Elemental analysis(%) calcd. for $C_{36}H_{28}ErN_3O_8$(**4**): C 54.19, H 3.53, N 5.27; found: C 54.52, H 3.48, N 5.40.

2.3 Crystal Structure Determination

The intensity data were collected on a Mercury CCD diffractometer with a graphite-monochromated Mo $K\alpha$(λ= 0.071073 nm) radiation at room temperature. All the absorption corrections were performed *via* SADABS program[16]. The structures were solved by direct methods and refined by full-matrix least squares on F^2 *via* SHELXL-97 program[17,18]. Non-hydrogen atoms were refined anisotropically, while hydrogen atoms were introduced in the calculated positions. The details of crystal data, collection and structure refinement of complexes **1—4** are listed in Table 1.

Table 1 Crystal data and structure refinement for complexes 1—4

Complex	**1**	**2**	**3**	**4**
Formula	$C_{36}H_{28}LaN_3O_8$	$C_{24}H_{19}EuN_2O_6$	$C_{24}H_{19}TbN_2O_6$	$C_{36}H_{28}ErN_3O_8$
M_r	769.52	583.37	590.33	797.87
Crystal system	Monoclinic	Monoclinic	Monoclinic	Orthorhombic
Space group	$P2_1/c$	$P2_1/c$	$P2_1/c$	$Ibca$
a/nm	0.9734(5)	0.37855(16)	0.37597(9)	0.95700(3)
b/nm	1.3643(7)	1.8079(8)	1.8081(4)	2.72074(10)
c/nm	2.6661(12)	3.0303(13)	3.0211(7)	2.75662(11)
β/(°)	104.482(1)	90.950(8)	91.381(5)	90
V/nm^3	3.428(3)	2.0736(1)	2.0531(8)	7.1775(4)
Z	4	4	4	8
ρ/(g·cm^{-3})	1.491	1.869	1.910	1.477
μ/mm^{-1}	1.301	3.071	3.492	2.391
F(000)	1544	1152	1160	3176
GOF on F^2	1.074	1.059	1.095	1.027
Collected reflection	31127	15812	15820	26332
Unique reflection(R_{int})	7792(0.0537)	4661(0.0595)	4606(0.0554)	4099(0.0258)
Observed reflection[$I>2(I)$]	5856	3795	3997	3223
Refined parameter	435	292	299	218
$R_1{}^a/wR_2{}^b$ [$I>2(I)$]	0.0499/0.1113	0.0390/0.0859	0.0421/0.1015	0.0257/0.0723
$R_1{}^a/wR_2{}^b$(all data)	0.0739/0.1228	0.0537/0.0940	0.0501/0.1074	0.0336/0.0785
CCDC No.	976409	976410	976411	976412

a. $R_1 = \sum||F_o|-|F_c||/\sum|F_o|$; *b*. $wR_2 = \{\sum[w(F_o^2-F_c^2)^2]/\sum[w(F_o^2)^2]\}^{1/2}$.

3 Results and Discussion

3.1 Syntheses

Hydrothermal synthesis has been proven to be a useful technique in the preparation of Ln CPs, especially when the solubility of the raw material in water is low. Since the solubilities of HL and Ln oxides are both low at normal pressure and temperature, hydrothermal method was utilized in the paper. The composition and purity of all the products were confirmed by elemental analyses, IR spectra and PXRD. And the results of elemental analyses are in good agreement with the formulas of complexes **1—4**. The characteristic features of carboxylate for all products are shown in the IR spectra (Fig.1). The observed experimental XRD patterns approximately match the simulated patterns generated from the single crystal data, which clearly confirm the phase purity of the bulk sample(Fig.2).

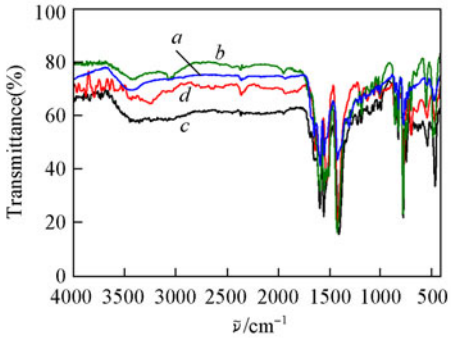

Fig.1 IR spectra of complexes 1—4(*a—d*)

3.2 Description of Crystal Structures

3.2.1 Crystal Structure of $LaL_3(H_2O)_2$(1)

The results of single-crystal X-ray analysis of complex **1** reveal it crystallizing in monoclinic space group $P2_1/c$. The asymmetric unit consists of one La^{3+} ion, three L ligands and two coordinated water molecules. La^{3+} ion exhibits distorted

bicapped trigonal prism geometry bridged by six carboxylate oxygen atoms(O_{COO}−) and two terminal water molecules. The bond distances of La—O vary from 0.2458(3) nm to 0.2654(4) nm, which are comparable to those of the related complexes[19,20]. La^{3+} ions are tetra- and double bridged by carboxylate groups of L ligands alternately in μ-L-κ^1O, κ^1O′ fashion(Scheme 1) to form a 1D linear chain along the *a* axis [Fig.3(A)]. Since the pyridyl nitrogen(N_{PY}) atoms are uncoordinated, the infinite La organic chains cannot extend to high-dimensional Ln coordination polymers. The parallel chains are linked by additional hydrogen bonds between water molecules and N_{PY} or O_{COO}− atoms[O1W—H1WB···N3: 0.2877(5) nm, 155.6°; O2W—H2WA···O3: 0.2937(5) nm, 139.4°] to give a supramolecular structure[Fig.3(B)].

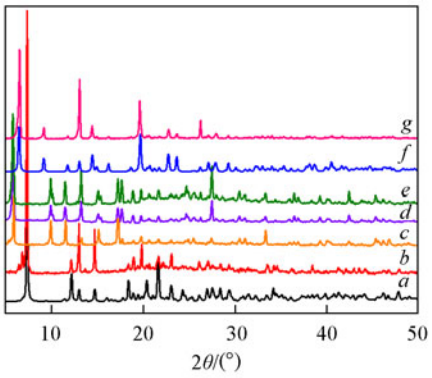

Fig.2 Simulated and experimental PXRD patterns of complexes 1—4

a. Simulated pattern of complex **1**; *b*. experimental pattern of complex **1**; *c*. simulated pattern of complex **2**; *d*. experimental pattern of complex **2**; *e*. experimental pattern of complex **3**; *f*. simulated pattern of complex **4**; *g*. experimental pattern of complex **4**.

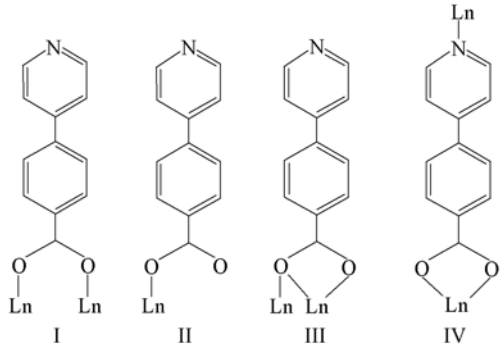

Scheme 1 Coordination modes of L ligands in complexes 1(I), 2 and 3(II—III), as well as 4(I, IV)

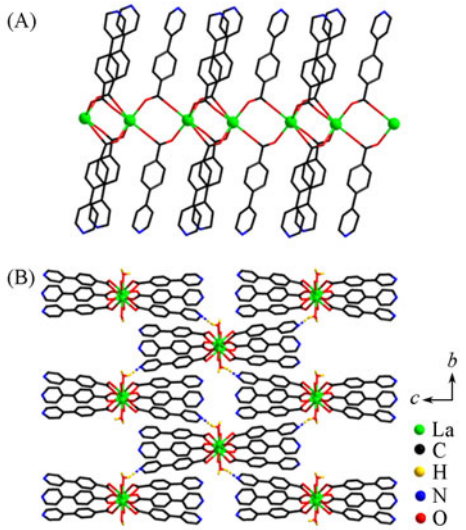

Fig.3 Ball-stick views of 1D La chain(A) and supramolecular structure(B) of complex 1

3.2.2 *Crystal Structure of $LnL_2(\mu_3$-OH)(H_2O)[Ln= Eu(2), Tb(3)]*

Complexes **2** and **3** are isostructural, so only the structure

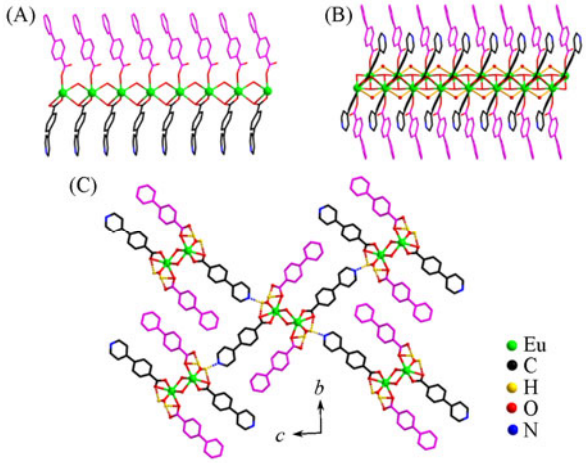

Fig.4 Ball-stick views of linear chain(A), ladder-like chain(B) and 3D supramolecular structure(C) of complex 2

L ligands in mode II and III are marked in pink and black for clarity.

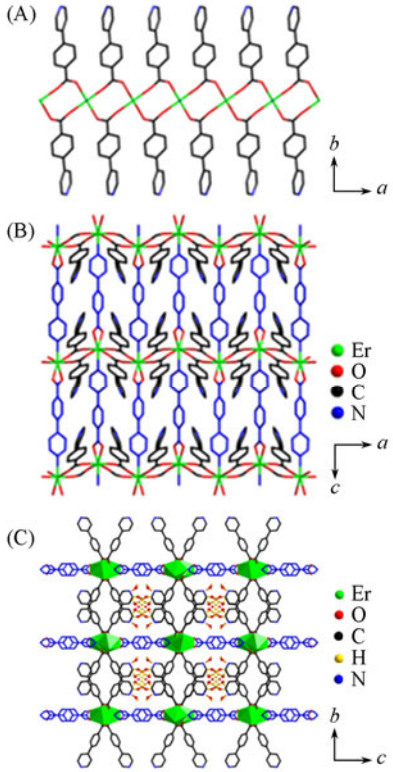

Fig.5 Wire views of 1D chain along *a* axis(A), the layer network viewing down along *b* axis(B) and 3D supramolecular structure(C) of complex 4

L ligands in mode I and IV are marked in black and blue for clarity.

of complex **2** was discussed in detail. The asymmetric unit of complex **2** contains one Eu^{3+} ion, two L ligands, one hydroxyl group and one bridging water molecule. Eu^{3+} ion is nine-coordinated with tricapped trigonal prism geometry enclosed by seven O_{COO}- atoms and two terminal water molecules. The bond distances of Eu—O[0.2363(3)—0.2629(3) nm] are in the normal range for Eu^{3+} ions[21], which are longer than the Tb—O distances[0.2340(3)—0.2618(4) nm] due to the lanthanide contraction effect[22]. Eu^{3+} ions are bridged by L ligands in mode III to form a linear chain along *a* axis[Fig.4(A)]. Additionally, pendant L ligands in mode II further stabilize the linear chain. A couple of paralleled chains are welded by hydroxyls to form a ladder-like chain[Fig.4(B)]. There are intramolecular hydrogen bond interactions between the coordination water molecules and the O_{COO}− atoms from the L ligands [O1W—H11···O1: 0.2772(4) nm, 113.4°; O1W—H12···O4: 0.2917(4) nm, 115.5°; O1W—H12···O5: 0.2635(4) nm, 173.9°]. Furthermore, there are interchain hydrogen bond interactions between the coordinated water molecules and the N_{PY} atoms from the L ligands[O1W—H11···N1: 0.2718(4) nm, 132.1°] [Fig.4(C)].

3.2.3 Crystal Structure of $ErL_3{\cdot}2H_2O$(4)

The results of single-crystal X-ray diffraction analysis is helpful to understanding the intrinsic subtle difference between complex **1** and complex **4** although they possess the same component. Different from chain structure of complex **1**, complex **4** crystallizes in orthorhombic space group *Ibca* with a 2D layer structure. Its asymmetric unit contains half Er^{3+} ion, one and a half L ligands, as well as one lattice water molecule. Er^{3+} ion is seven-coordinated with capped trigonal prism geometry bridged by six O_{COO}− atoms and one N_{PY} atom. The bond distances of Er—O are in a range of 0.2203(2)—0.2500(4) nm, which are accorded with those of the related complexes[8,23]. Er^{3+} ions are connected by L ligands in mode I, generating one 1D chain along *a* axis[Fig.5(A)]. Such corrugated chains are further linked by L ligand in mode IV to form a 2D grid layer on *ac* plane[Fig.5(B)]. From the topology point of view, such a layer can be regarded as a 4-connected *sql* tetragonal plane net with the Schläfli symbol($4^4.6^2$)[24]. The parallel layers with a distance of about 1.3783 nm are linked by additional hydrogen bonds[O3W—H3WA···N1: 0.332(19) nm, 138.5°; O3W—H3WB···O2W: 0.28(2) nm, 165.9°] to give a supramolecular structure[Fig.5(C)].

3.3 Thermogravimetric Analyses

To study the thermal stability of all the complexes, TG analyses were carried out. As shown in Fig.6, all the complexes undergo two stages of mass losses. The first mass loss from 30 °C to 300 °C is attributed to the removal of the lattice/coordination water molecules as well as hydroxyls for complex **1**: calcd. 4.7%, found 4.9%; complex **2**: calcd. 6.1%, found 5.9%; complex **3**: calcd. 6.2%, found 5.9%; complex **4**: calcd. 4.5%, found 4.7%. The rest mass losses correspond to the successive release of organic ligands. When the temperature reaches 600 °C, all the Ln CPs decompose completely. Assuming that the residue corresponds to Ln_2O_3, the observed masses are in good agreement with the calculated ones for complexes **1**—**4**: complex **1**: calcd. 21.2%, found 21.5%; complex **2**: calcd. 30.2%, found 30.4%; complex **3**: calcd. 31.1%, found 31.3%; complex **4**: calcd. 24.6%, found 24.8%.

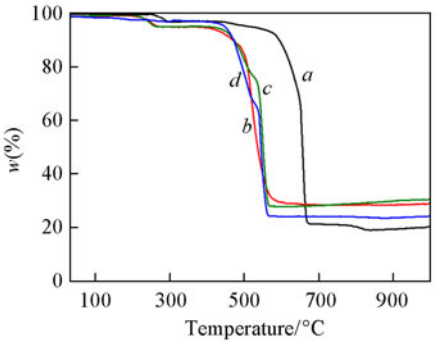

Fig.6 TG curves of complexes 1—4(*a*—*d*)

3.4 Luminescent and Optical Properties

In view of the fact that Ln CPs have high color purity and high quantum, the solid-state luminescent properties of complexes **2** and **3** were measured at room temperature with photoexcitation at 320 and 378 nm, respectively(Fig.7). Complex **2** displays intense red luminescence and exhibits the characteristic transition of $^5D_0\rightarrow{}^7F_J$(J=0—4) of Eu^{3+} ion[21,25]. The strongest emission bands located at about 616 and 594 nm are assigned to $^5D_0\rightarrow{}^7F_2$ and $^5D_0\rightarrow{}^7F_1$ transitions, respectively, which are sensitive to the symmetry of the coordination sphere of Eu^{3+} ion. The intensity ratio of $^5D_0\rightarrow{}^7F_2$ transition to $^5D_0\rightarrow{}^7F_1$ transition indicates the absence of inversion symmetry center and the low symmetry of Eu^{3+} site[26], which are in agreement with the distorted tricapped trigonal prism coordination environment. Complex **3** yields intense green luminescence and exhibits characteristic transition of $^5D_4\rightarrow{}^7F_J$(J=3—6) of Tb^{3+} ion[27,28]. The two most intense emission bands found

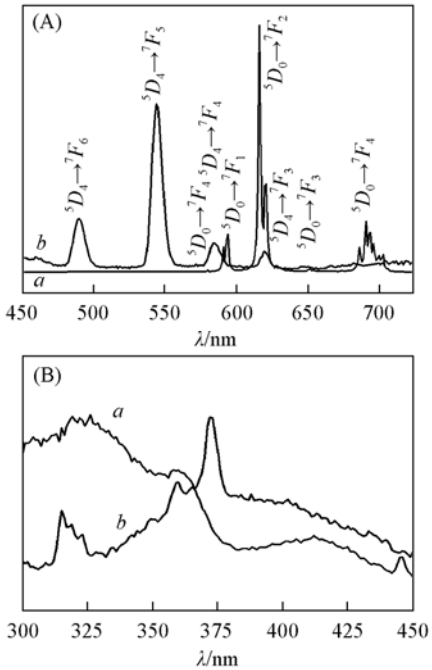

Fig.7 Emission(A) and excitation(B) spectra of complexes 2(*a*) and 3(*b*)

at about 490 and 544 nm correspond to $^5D_4 \rightarrow {}^7F_6$ and $^5D_4 \rightarrow {}^7F_5$ transitions, respectively, while the weaker emission bands at 585 and 619 nm are originated from $^5D_4 \rightarrow {}^7F_4$ and $^5D_4 \rightarrow {}^7F_3$ transitions. To further investigate the optical properties of these two complexes, UV-Vis diffuse reflectance spectra of them were measured. The results of the optical diffuse reflectance studies reveal that the band gaps of complexes **2** and **3** are 3.90 and 3.93 eV, respectively(Fig.8).

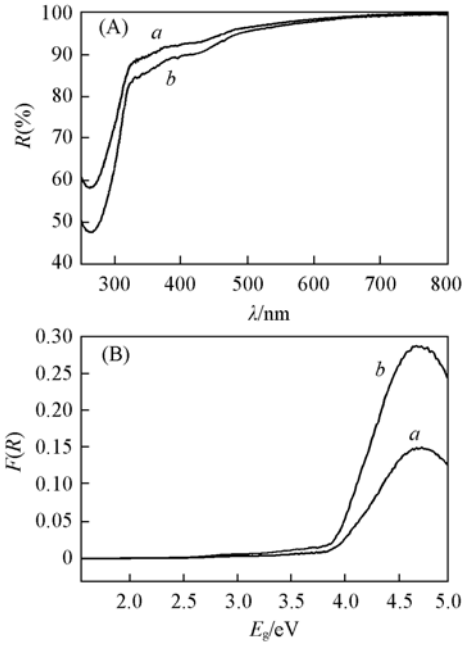

Fig.8 UV-Vis optical diffuse reflectance spectra(A) and band gaps(B) of complexes 2(*a*) and 3(*b*)

4 Conclusions

Different ratios of initial reactants and different conditions of hydrothermal reactions lead to the formation of four different Ln coordination polymers. The progressive structural variation from linear chain(**1**) to ladder-like chain(**2**, **3**) and to layered network(**4**) is attributed to the difference of material ratios, the lanthanide contraction effect and the coordination modes of L ligands. In addition, red and green luminescence could be observed for complexes **2** and **3**. Further studies on the syntheses of novel Ln CPs with fascinating structures and properties are undergoing.

Supplementary Material

CCDC 976409—976412 contains the supplementary crystallographic data for this paper. These data can be obtained free of charge via www.ccdc.cam.ac.uk/conts/retrieving.html(or from the Cambridge Crystallographic Data Centre, 12 Union Road, Cambridge CB2 1EZ, UK; fax: (+44)1223-336-033; or e-mail: deposit@ccdc.cam.ac.uk).

References

[1] Yaghi O. M., O'Keeffe M., Ockwig N. W., Chae H. K., Eddaoudi M., Kim J., *Nature*, **2003**, *423*, 705
[2] Kagan H. B., *Chem. Rev*., **2002**, *102*, 1805
[3] Rocha J., Carlos L. D., Paz F. A., Ananias D., *Chem. Soc. Rev.*, **2011**, *40*, 926
[4] Zhao X. Q., Wang H., Dong L. J., Xu Q. H., *Chem. J. Chinese Universities*, **2013**, *34*(6), 1318
[5] Benelli C., Gatteschi D., *Chem. Rev*., **2002**, *102*, 2369
[6] Khan N. H., Kureshy R. I., Abdi S. H. R., Agrawal S., Jasra R. V., *Coord. Chem. Rev*., **2008**, *252*, 593
[7] Zhang M. B., Zhang J., Zheng S. T., Yang G. Y., *Angew. Chem. Int. Ed*., **2005**, *44*, 1385
[8] Cheng J. W., Zhang J., Zheng S. T., Zhang M. B., Yang G. Y., *Angew. Chem. Int. Ed*., **2006**, *45*, 73
[9] Cheng J. W., Zheng S. T., Liu W., Yang G. Y., *CrystEngComm*, **2008**, *10*, 1047
[10] Huang Y. G., Jiang F. L., Hong M. C., *Coord. Chem. Rev*., **2009**, *253*, 2814
[11] Fang W. H., Cheng L., Huang L., Yang G. Y., *Inorg. Chem*., **2013**, *52*, 6
[12] Fang W. H., Wang Z. L., Yang G. Y., *Chin. J. Inorg. Chem*., **2010**, *26*, 1917
[13] Wang Z. L., Fang W. H., Yang G. Y., *J. Cluster Sci*., **2009**, *20*, 725
[14] Fang W. H., Wang Z. L., Yang G. Y., *J. Cluster Sci*., **2010**, *21*, 187
[15] Wang Z. L., Fang W. H., Yang G. Y., *Chinese J. Struct. Chem*., **2009**, *28*, 1453
[16] Sheldrick G. M., *SADABS, Program for Siemens Area Detector Absorption Corrections*, University of Göttingen, Göttingen, **1997**
[17] Sheldrick G. M., *SHELXL-97, Program for Crystal Structure Refinement*, University of Göttingen, Göttingen, **1997**
[18] Sheldrick G. M., *SHELXS-97, Program for Crystal Structure Solution*, University of Göttingen, Göttingen, **1997**
[19] Fu J., Zheng L., Zhang Z., Xu Y., *Inorg. Chim. Acta*, **2012**, *383*, 112
[20] Wang S. H., Hu H. Z., Chen C., Ma R. N., Zhang N., *Chem. J. Chinese Universities*, **2014**, *35*(10), 2055
[21] Sun Y. Q., Zhang J., Chen Y. M., Yang G. Y., *Angew. Chem. Int. Ed*., **2005**, *44*, 5814
[22] Pan L., Huang X., Li J., Wu Y., Zheng N., *Angew. Chem. Int. Ed*., **2000**, *39*, 527
[23] Zhang Y., Chen L., Ju. W. W., Xu Y., *Chem. Res. Chinese Universities*, **2014**, *30*(2), 194
[24] Blatov V. A., Shevchenko A. P., Proserpio D. M., *Cryst. Growth Des*., **2014**, *14*, 3576
[25] Sun Y. Q., Zhang J., Yang G. Y., *Chem. Commun*., **2006**, 1947
[26] Kirby A. F., Foster D., Richardson F. S., *Chem. Phys. Lett.*, **1983**, *95*, 507
[27] Cheng J. W., Zheng S. T., Yang G. Y., *Dalton Trans*., **2007**, 4059
[28] Yan W. M., Long J. F., Fu Z. Y., Rui F., Lian C., Chun H. M., *Inorg. Chem. Commun*., **2012**, *15*, 25